

## The Effect of Wavy Leading Edge Modifications on NACA 0021 Airfoil Characteristics

N. Rostamzadeh, R.M. Kelso, B.B. Dally and K.L. Hansen

School of Mechanical Engineering

University of Adelaide, Adelaide, South Australia 5005, Australia

### Abstract

In spite of its mammoth physical size, the Humpback whale's manoeuvrability in hunting has captured the attention of biologists as well as fluid mechanists. It has now been established that the protrusions on the leading edges of the Humpback's pectoral flippers, known as tubercles, account for this baleen species' agility. In the present work, Prandtl's non-linear lifting-line theory was employed to propose a hypothesis that the favourable traits observed in the performance of tubercled lifting bodies are not exclusive to this form of leading edge configuration. Accordingly, a novel alternative to tubercles was introduced and incorporated into the design of four airfoils that underwent wind tunnel force measurement tests in the transitional flow regime. The experimental results demonstrate similar loading characteristics of the newly designed foils in comparison with those with tubercles, suggesting the presence of an analogous flow mechanism.

### Introduction

The Humpback whale's dynamic agility in executing tight turns when catching prey is remarkable [10]. When rolling in a banking turn, hydrodynamic lift forces are developed on the Humpback's flippers whose horizontal components act as the centripetal force [17]. Fish and Battle [6] postulated that the protuberances on the leading edges of the whale's pectoral flippers, known as tubercles, may account for the Humpback's extraordinary manoeuvrability through maintaining lift at high attack angles.

To assess the hypothesis, Miklosovic *et al.* [12] conducted a series of wind tunnel experiments that unveiled the desirable characteristics of idealised flipper models. It was learned that, compared to the finite-span wing without tubercles, the modified model delayed the stall angle by nearly 40%, achieved a 6% increase in the maximum lift coefficient and incurred lower drag at high incidence angles.

Inspired by the initial promising results, Stein *et al.* [15], Miklosovic *et al.* [11], Johari *et al.* [9] and Hansen *et al.* [7] carried out low Reynolds number force measurement tests on nominally two-dimensional foils, as opposed to finite wings. It was found that, compared to the unmodified models, most foils with tubercles displayed gradual stall characteristics with higher post-stall lift, yet their pre-stall performance was degraded.

Amongst other studies, Custodio [4], van Nierop *et al.* [16], Stanway [14], Pedro and Kobayashi [13], and Hiroshi *et al.* [8] utilised experimental and numerical methods to examine the flow field around foils and wings with tubercles. An important outcome of these investigations indicated the presence of pairs of counter-rotating streamwise vortices in the vicinity of the lifting surfaces. Hence, it was proposed that the beneficial aspects of lifting surfaces with tubercles are associated with streamwise vorticity present in the flow field.

Although the desirable features of tubercles have been identified for full-span and semi-span wings, the underlying mechanisms and the role played by streamwise vortices through which these traits become manifest are not fully understood. In addition, leading edge modifications as alternatives to tubercles that trigger similar flow mechanisms have not been introduced.

In an attempt to gain further insight into the underlying flow dynamics induced by tubercles, Prandtl's non-linear lifting-line theory (PNLLT) was used in the present work. The analysis of span-wise circulation led to the design of a novel leading-edge configuration referred to as the wavy model. The hypothesis adopted was that the alternative modification would exhibit similar aerodynamic traits as predicted by PNLLT. Accordingly, four modified NACA 0021-based airfoils were fabricated to undergo wind tunnel force measurement tests in the transitional flow regime.

### Overview of Prandtl's Non-linear Lifting-line Theory

Ludwig Prandtl (1875-1953) in his classical lifting-line theory presented an innovative approach that enabled the study of significant aerodynamic parameters such as circulation and its distribution along the span of a finite wing [2, 5]. The non-linear lifting-line method as detailed by Anderson [1] is an extension of Prandtl's lifting-line theory with an advantage over a linear approach, as it incorporates experimental data associated with a baseline foil to capture the near and post-stall behaviour of a finite wing. Despite being an approximate method, in the context of wings with passive undulating leading edges, the iterative PNLLT scheme can shed light on the development of circulation.

### Details of Analysis

Herein, two forms of wings with undulating leading edges were considered: tubercles, where the chord varies in a sinusoidal manner along the span of a finite wing [2, 5]. The non-linear lifting-line method as detailed by Anderson [1] is an extension of Prandtl's lifting-line theory with an advantage over a linear approach, as it incorporates experimental data associated with a baseline foil to capture the near and post-stall behaviour of a finite wing. Despite being an approximate method, in the context of wings with passive undulating leading edges, the iterative PNLLT scheme can shed light on the development of circulation.

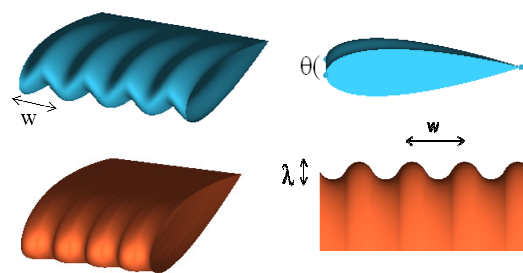


Figure 1. Top row: Wavy wing section showing peak-to-peak angular amplitude and wavelength. Bottom row: Tubercled wing section showing the amplitude and wavelength

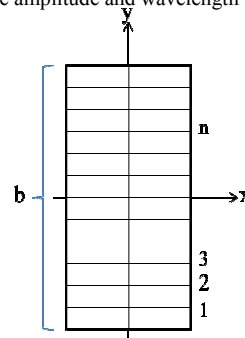


Figure 2. The coordinates system with a number of stations marking various locations along the span (top view)

Each wavelength of the wing was allocated a number of stations to represent various locations along the span (Figure 2). As an initial estimate, an elliptic lift distribution was assigned to the stations according to:

$$\Gamma(y_n)_{\text{initial}} = \Gamma_0 \sqrt{1 - \left(\frac{2y_n}{b}\right)^2} \quad (1)$$

$\Gamma_0$ , an arbitrary initial guess, was set to  $0.4 \text{ (m}^2\text{s}^{-1}\text{)}$ .

The induced angle of attack was found by:

$$\alpha_i(y_n) = \frac{1}{4\pi V_\infty} \int_{-b/2}^{b/2} \frac{d\Gamma/dy}{y_n - y} dy \quad (2)$$

where  $V_\infty = 25 \text{ (ms}^{-1}\text{)}$  is the free-stream speed and  $b=0.495 \text{ (m)}$  is the span. These values were chosen to match the parameters in the present work's experimental setup.

Next, Simpson's rule was applied to compute the integral in (2):

$$\frac{\alpha_i(y_n)}{\zeta} = \sum_{j=2,4,6,8\dots}^k \frac{(d\Gamma/dy)_{j-1}}{(y_n - y_{j-1})} + 4 \frac{(d\Gamma/dy)_j}{(y_n - y_j)} + \frac{(d\Gamma/dy)_{j+1}}{(y_n - y_{j+1})} \quad (3)$$

$$\zeta = \frac{\Delta y}{12\pi V_\infty} \quad (4)$$

Singularities occur at  $(y_n = y_{j-1}, y_n = y_j, y_n = y_{j+1})$ . Therefore, these terms had to be estimated using the average of the neighbouring terms [1]. For instance, at  $(y_n = y_{j-1})$ :

$$2 \frac{(d\Gamma/dy)_{j-1}}{(y_n - y_{j-1})} = \frac{(d\Gamma/dy)_{j-2}}{(y_n - y_{j-2})} + \frac{(d\Gamma/dy)_j}{(y_n - y_j)} \quad (5)$$

For a wavy wing, the geometric angle of attack is given by:

$$\alpha_n = \frac{\theta}{2} \sin\left(\frac{2\pi}{w} y_n\right) \quad (6)$$

By contrast, for tubercles, the chord varies according to:

$$c_n = \frac{\lambda}{2} \sin\left(\frac{2\pi}{w} y_n\right) + c_{\text{mean}} \quad (7)$$

$c_{\text{mean}} = 0.07 \text{ (m)}$  is the mean chord. Given the geometric attack angle and the calculated induced angle in equation (2) at each station, the effective angle of attack was obtained by Prandtl's *Fundamental equation of lifting-line theory*:

$$\alpha_E = \alpha - \alpha_i \quad (8)$$

At each station, the value of the effective attack angle was used to extract the baseline NACA0021 lift coefficient, obtained from experimental data by Hansen *et al.*[7].

Using the Kutta-Joukowski's theorem, a new circulation distribution was found from the lift coefficient distribution:

$$\Gamma_n = \frac{1}{2} V_\infty c_n (C_L)_n \quad (9)$$

The circulation distribution was then compared to the initial guess and updated in (9) where a typical value of 0.04 was selected for the damping coefficient,  $\varepsilon$ .

$$\Gamma_{\text{new}} = \Gamma_{\text{initial}} + \varepsilon(\Gamma_{\text{initial}} - \Gamma_n) \quad (10)$$

Subsequently, a loop was established by replacing  $\Gamma_{\text{initial}}$  with  $\Gamma_{\text{new}}$  in equation (1). Convergence was determined once the difference between two consecutive estimates of circulation at each station diminished to 0.001.

## Results of Theoretical Analysis

Figure 3 (a-d) illustrates how circulation varies along half of the span for a tubercled and a wavy wing pre- and post-stall. The values for wavelength and amplitude are expressed in millimetres, and the peak-to-peak amplitude in degrees.

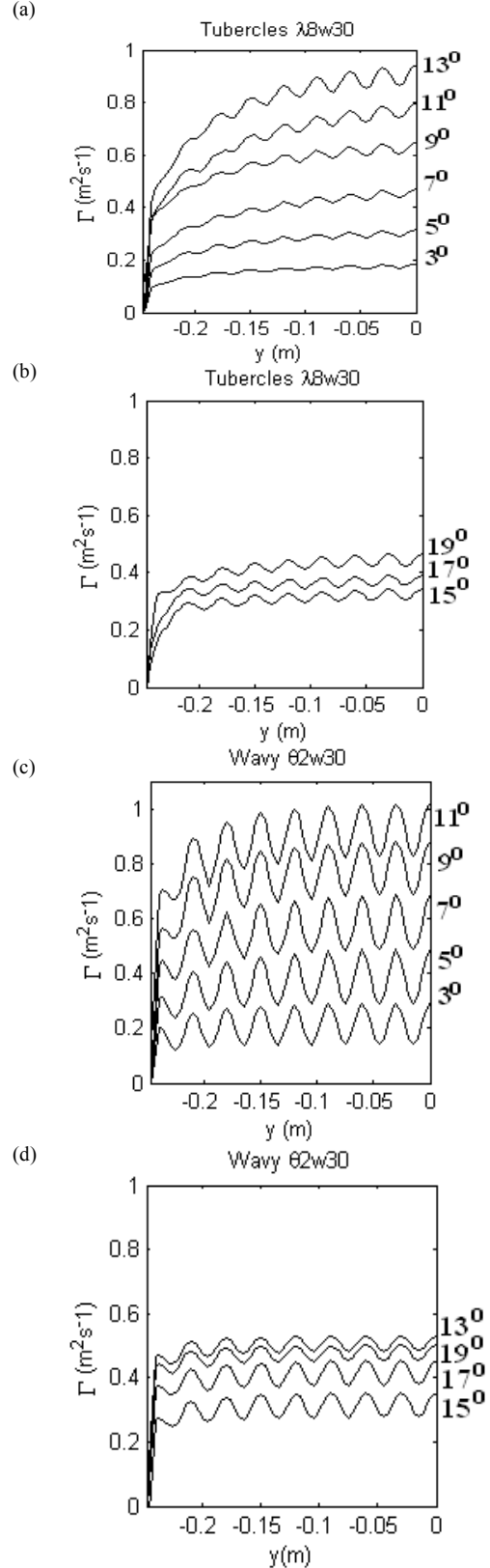


Figure 3 (a-d). Spanwise circulation for a tubercled and wavy foil at various incidence angles along half of the span

To predict the effect of the peak-to-peak angular amplitude and wavelength on the overall performance of wavy wings, circulation was integrated along the span for three finite wings:

$$C_L = \frac{2}{V_\infty b} \int_{-b/2}^{b/2} \Gamma(y) dy \quad (11)$$

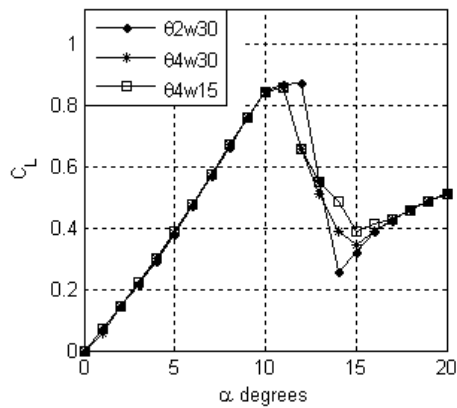


Figure 4. Lift coefficient for three finite wavy wings obtained by Prandtl's non-linear lifting-line theory

Prandtl's non-linear lifting-line theory demonstrates that, for the wavy wing, the distribution of circulation along the span assumes an oscillatory pattern similar to that of tubercles, pointing to the presence of streamwise vortices in both cases. It is also noticed that with the increase in attack angle, the amplitude of oscillations grows for the tubercled wing. Since the strength of the streamwise vortices is proportional to the slope of the circulation curve, it is predicted that stronger vortices are generated at higher attack angles. On the other hand, for the wavy wing, the amplitude of oscillations is noticeably larger even at low angles, signifying the presence of stronger vortices.

As illustrated in Figure 4, the wavy wing with  $\theta = 2(\text{deg})$  undergoes sudden stall while the ones with  $\theta = 4(\text{deg})$  experience a more gradual loss of lift. It is also predicted that ( $\theta 4w15$ ) would stall less abruptly compared to wings with wavelengths equal to 30 (mm). From these observations, it can be deduced that wavy wings with shorter wavelengths and larger peak-to-peak amplitudes are likely to display more desirable attributes such as extended and gradual stall.

Although the results presented here are derived for finite-wings, it is conceivable that the global behaviour of spanwise circulation for full-span lifting surfaces is oscillatory.

### Details of Experimental Work

To assess the aerodynamic loading characteristics of full-span wavy foils against an unmodified model, a series of force measurement tests were performed at  $Re=120,000$  in the closed-loop KC wind tunnel at the University of Adelaide. The test section of the tunnel has a  $500(\text{mm}) \times 500(\text{mm})$  cross-section with a maximum blockage ratio of 6% at a 25-degree attack angle. The turbulent intensity of the tunnel is approximately 0.8% ahead of the test subject.

Of the four NACA0021-based wavy foils with varying wavelength and peak-to-peak angular amplitude, three were machined from aluminium and one was cast from epoxy resin (Figure 5). All the airfoils have mean chord and span lengths equal to 70 (mm) and 495 (mm) respectively.

A six-component load cell from JR3, with an uncertainty estimate of  $\pm 1\%$ , was used to measure normal and chord-wise forces (with respect to the airfoil) which were then converted into lift and drag. A Vertex rotary table was attached to the base

of the load cell to allow accurate and repeatable changes in the attack angle.

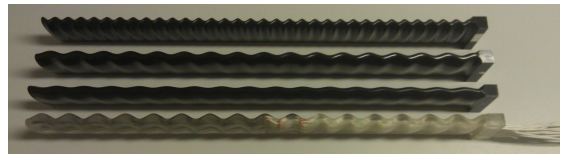


Figure 5. Wavy foils :  $\theta 4w15$  ,  $\theta 4w30$  ,  $\theta 2w30$  ,  $\theta 6.5w30$  (top to bottom)

With the sampling period of the analogue-to-digital converter set to 16 (ms), 3,000 data points, corresponding to normal and tangential force components, were collected at each angle of attack. The tests were repeated five times for every foil and average values of the lift and drag coefficients were calculated accordingly. The average standard errors in estimating the population means for lift and drag coefficients were 0.003 and 0.009. Wind tunnel corrections for solid, wake blockage and streamline curvature were also applied to the results in accordance with recommendations by Barlow[3].

### Experimental Results

#### Performance Effect of Variation in Wavy Foil Wavelength

It is noticed from Figure 6, that the unmodified and wavy foils produce nearly the same lift-curve slope up to 4 degrees. At this point, the curves deviate from the linear trend which hints at extra lift produced by the presence of laminar separation bubbles (LSB). With regard to the maximum lift coefficient, the unmodified foil achieves the highest value, followed by a dramatic loss of lift past 12 degrees, and a consequent rise in drag.

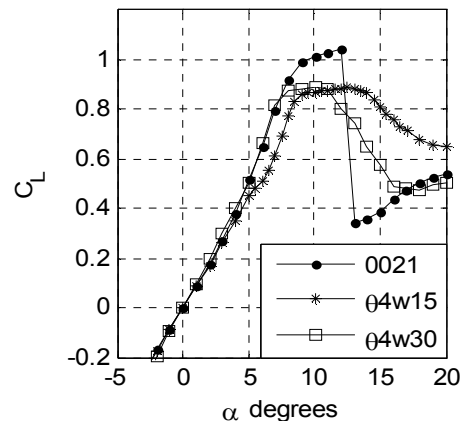


Figure 6. Lift coefficient versus attack angle for two wavy foils of varying wavelength, and the unmodified NACA 0021

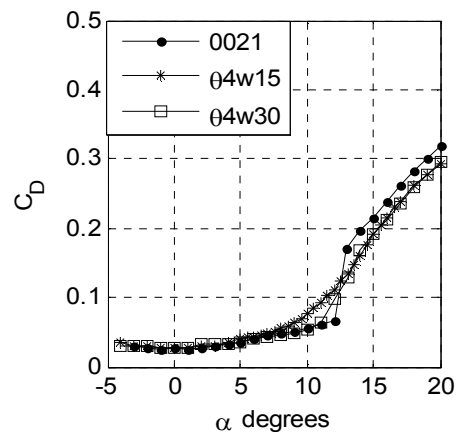


Figure 7. Drag coefficient versus angle of attack for two wavy foils of varying wavelength, and the unmodified NACA0021

Between the wavy foils of the same wavelength,  $\theta 4w15$  outperforms  $\theta 4w30$  post-stall as it undergoes a more gradual stall with a higher amount of lift, indicating that smaller wavelengths may be more beneficial for wavy foils.

#### Performance Effect of Variation in Wavy Foil Peak-to-Peak Angular Amplitude

Comparison of the lift coefficient for the wavy foils of the same wavelength against the unmodified NACA 0021 foil (Figures 8 and 9) reveals that both wavy foils produce lower lift pre-stall. The unmodified and  $\theta 2w30$  foils exhibit a sudden loss of lift and identical post-stall behaviour, however  $\theta 6.5w30$  shows superior performance past 12 degrees with lower drag coefficients. The observations indicate that wavy foils with higher peak-to-peak amplitudes may render more aerodynamic benefits in the post-stall region.

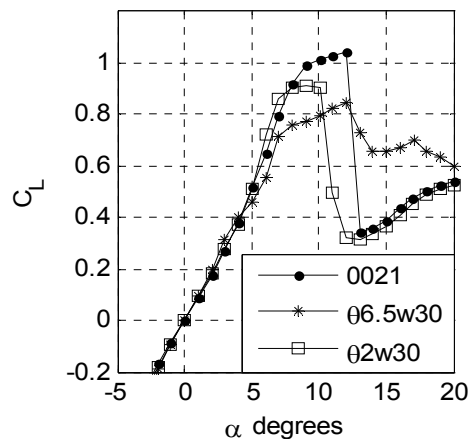


Figure 8. Lift coefficient versus the attack angle for two wavy foils of varying peak-to-peak angular amplitude, and the unmodified NACA 0021

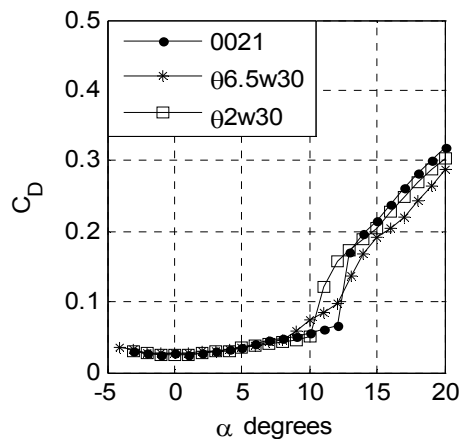


Figure 9. Drag coefficient versus the attack angle for two wavy foils of varying peak-to-peak angular amplitude, and the unmodified NACA 0021

#### Conclusions

The present investigation attempted to broaden our understanding of the flow mechanism triggered by incorporating passive leading edges. In spite of its simplified assumptions, Prandtl's non-linear lifting-line theory succeeded in demonstrating that both the newly-proposed design, referred to as the wavy configuration, and tubercles, induce an oscillatory distribution of circulation along the span. This prediction implies that the wavy foils exhibit similar aerodynamic characteristics to those with tubercles. In addition,

the pattern of circulation points to the presence of streamwise vortices in flows over wavy lifting surfaces.

The results of wind tunnel tests on four wavy foils revealed that three of the wavy foils showed delayed stall, a prominent trait also observed in flows over tubercled wings. Amongst the examined models, the one with the highest peak-to-peak angular amplitude and smallest wavelength yielded the most favourable post-stall behaviour. In view of the findings, there is sufficient evidence to merit more attention to the proposed novel leading edge modification.

#### Acknowledgements

Thanks to Mechanical Engineering workshop staff, in particular Mr. Bill Finch and Mr. Richard Pateman, for their valuable cooperation in the process of manufacturing the wing models.

#### References

1. Anderson, J., *Fundamentals of Aerodynamics*. Fourth ed. 2005: McGraw-Hill International Higher Education.
2. Anderson, J.D., Corda, S., and Van Wie, D.M., *Numerical Lifting Line Theory Applied to Drooped Leading-Edge Wings Below and Above Stall*. Journal of Aircraft, 1981. **17**(12).
3. Barlow, J.B., Pope, A., and Rae, W.H., *Low Speed Wind Tunnel Testing*. 3rd edition (September 1999): Wiley-Interscience.
4. Custodio, D., *The Effect of Humpback Whale-Like Leading Edge Protuberances on Hydrofoil Performance*, in Thesis submitted to Worcester Polytechnic Institute. December 2007.
5. Durrand, W.F., *Aerodynamic Theory*. Vol. 1 and 2. 1935, Berlin: Julius Springer.
6. Fish, F.E. and Battle, J.M., *Hydrodynamic Design of the Humpback Whale Flipper*. Journal of Morphology, 1995. **225**: p. 51-60.
7. Hansen, K.L., Kelso, R.M., and Dally, B.B., *Performance variations of leading-edge tubercles for distinct airfoil profiles*. AIAA Journal Journal of Aircraft, 2011. **49**:185-94.
8. Hiroshi, A., et al., *A Study on Stall Delay by Various Wavy Leading Edges*. Journal of Aero Aqua Bio-mechanisms, 2010. **1**(Special Issue on Fourth International Symposium on Aero Aqua Bio-Mechanisms): p. 18-23.
9. Johari, H., et al., *Effects of Leading Edge Protuberances on Airfoil Performance*. AIAA Journal, November 2007. **45**:11.
10. Jurasz, C.M. and Jurasz, V.P., *Feeding Modes of the Humpback Whale, Megaptera novaeangliae, in Southeast Alaska*. Scientific Reports of the Whales Research Institute, 1979. **31**: p. 69-83.
11. Miklosovic, D.S., Murray, M.M., and Howle, L., *Experimental Evaluation of Sinusoidal Leading Edges*. Journal of Aircraft, 2007. **44**:1404-1407.
12. Miklosovic, D.S., et al., *Leading Edge Tubercles Delay Stall on Humpback Whale Flippers*. Physics of Fluids, 2004. **16**(5) : p. L39-L42.
13. Pedro, H.T.C. and Kobayashi, M.H. *Numerical Study of Stall Delay on Humpback Whale Flippers*. in Proceedings of 46th AIAA Aerospace Sciences Meeting and Exhibit. 7-10 January 2008. Reno, Nevada.
14. Stanway, M.J., *Hydrodynamic effects of leading-edge tubercles on control surfaces and in flapping foil propulsion*, in Mechanical Engineering. February 2008, Massachusetts Institute of Technology.
15. Stein, B. and Murray, M.M. *Stall Mechanism Analysis of Humpback Whale Flipper Models*. in Proc. of Unmanned Untethered Submersible Technology (UUST). August 2005. Durham, NH.
16. van Nierop, E., Alben, S., and Brenner, M.P., *How Bumps on Whale Flippers Delay Stall: an Aerodynamic Model*. Physical review letters, 7 February 2008. **PRL 100**: 054502.
17. Weihs, D., *Effects of Swimming Path Curvature on the Energetics of Fish Swimming*. Fish Bull, 1981. **79**: p. 171-176.